Optical properties of incommensurately modulated calaverite, AuTe2

Loosdrecht, P.H.M. van; Gerrits, A.M.; Balzuweit, K.; König, W.; Wittlin, A.; Bentum, P.J.M. van

Published in:
Default journal

DOI:
10.1088/0953-8984/5/23/025

Publication date:
1993

J. Phys.: Condens. Matter 5 (1993) 3977–3986. Printed in the UK

Optical properties of incommensurately modulated calaverite, $AuTe_2$

P H M van Loosdrecht†, A M Gerrits†, K Balzuweit†, W König‡, A Wittlin† and P J M van Bentum†

† High Field Magnet Laboratory and Research Institute of Materials, University of Nijmegen, Toernooiveld, NL-6525 ED Nijmegen, The Netherlands

‡ MPI für Festkörper Forschung, Heisenbergstrasse 1, 7000 Stuttgart 1, Federal Republic of Germany

Received 3 February 1993, in final form 24 March 1993

Abstract. The optical reflection spectrum of incommensurately modulated calaverite is presented. Using a Kramers–Kronig analysis the dielectric function is derived from the reflection spectrum. The results for the imaginary part of the dielectric function are qualitatively discussed in terms of absorption by phonon, free electron and interband scattering. The phonon contribution clearly shows the influence of the incommensurability by the activity of phonons with $k \neq 0$. The free electron scattering can be understood in terms of a simple Drude model. The interband scattering is found at a lower frequency than predicted from electronic band structure calculations.

1. Introduction

Natural calaverite ($Au_{1-p}Ag_pTe_2$, $p < 0.15$) is a mineral ore which belongs to the class of displacively modulated incommensurate materials. As has been shown recently, the relatively large amplitude of the modulation wave in this material has a strong influence on its physical properties. Dam *et al* [1] have shown that the complex morphology is easily understood if one fully accounts for the incommensurability of $Au_{1-p}Ag_pTe_2$. In Raman experiments it was found that scattering processes involving $k = \pm lq$ ($l = 1, 2$), activated due to the incommensurate modulation, are important in the understanding of the vibrational spectra of $AuTe_2$ [2]. Optical experiments by Dijkstra *et al* [3] indicate that calaverite is optically active, despite the fact that it is centrosymmetric. It was argued that the optical activity might be due to the incommensurability of $Au_{1-p}Ag_pTe_2$.

In the incommensurate phase the structural symmetry of calaverite is given by the superspace-group $PC2/m(\alpha, 0, \gamma)\bar{1}s$, with the modulation wave vector $q = -0.408a^* + 0.448c^*$ [4]. The cell parameters of the average structure are $a = 7.19$ Å, $b = 4.40$ Å, $c = 5.07$ Å and $\beta = 90.04°$ [5]. At ambient pressure calaverite does not exhibit any structural phase transition with changing temperature. The modulation wave vector is approximately temperature independent below 400 K [4]. At higher temperature the modulation wave vector becomes slightly temperature dependent [6]. Pressure dependent x-ray experiments [7] have shown that at ~ 25 kbar ($T = 300$ K) a phase transition occurs to a commensurate cubic structure. This simple cubic structure is also found in crystals which are produced by a temperature quenching method [8]. It has been shown that these quenched cubic crystals are superconducting with a transition temperature of $T = 2.5$ K. The fact that cubic calaverite becomes superconducting might give an explanation of

0953-8984/93/233977+10$07.50

the superconductivity observed in incommensurate calaverite in point-contact experiments. Meekes *et al* [9] observed that $AuTe_2$–$AuTe_2$ point contacts become superconducting below $T = 2.3$ K and that Ag $AuTe_2$ point contacts exhibit characteristics reminiscent of Andreev reflection, even though bulk incommensurate calaverite is not a superconductor. It seems very possible that the pressure needed to produce the point contact locally induces a phase transformation to the cubic phase leading to the observed superconducting properties.

The presence of a modulation wave in a conductor leads to the formation of small additional gaps in the electronic band structure, besides the usual gaps induced by the lattice periodicity. In an incommensurately modulated conductor there is an infinitely large number of these gaps, formed whenever $\boldsymbol{k} = \pm l\boldsymbol{q} + \boldsymbol{K}$ ($l = 1, 2, \ldots$) [10], where $\boldsymbol{q}$ is the modulation wave vector, and $\boldsymbol{K}$ a reciprocal lattice vector. The magnitude of these gaps is expected to decrease strongly with increasing l. This leads to a distribution of small gaps, with the largest gaps formed for $\boldsymbol{k} = \pm\boldsymbol{q}$. Infrared experiments in chromium have shown the existence of at least the first-order gap, with a magnitude of 125 meV [11]. In addition, the zero-bias anomaly in point-contact experiments on Cr shows the existence of this gap, with a reported value of 110 meV [12].

The interest of the present paper concerns both the vibrational and the electronic properties of incommensurately modulated calaverite. These properties are probed using reflection spectroscopy over a wide frequency range in order to be able to derive the frequency dependence of the complex dielectric constant. One of the aims is to extract the electronic interband contribution to the optical spectra in order to investigate the possible existence of minigaps near the Fermi surface induced by the incommensurate modulation. The results are compared to existing experimental and theoretical literature data.

2. Experimental details

The crystals used in the experiments have been grown using the Kyropoulos technique with a magnetic pulling system as described elsewhere [13]. An SEM microprobe analysis of the purity of our samples, limited by the accuracy of our experimental set-up (1%), showed that the impurity level at the surface of our samples was below 1%.

The reflection experiments were performed on the natural surfaces (~ 8 mm^2) of the obtained crystals. For the infrared measurements the samples were mounted in a dynamic flow cryostat using polyethylene windows in the far-infrared region and KRS5 and ZnSe windows in the mid-infrared region. A gold mirror has been used as a reference material. The spectra are recorded using a BRUKER IFS 113V FT-IR spectrometer using unpolarized light. A KBr beamsplitter and Mylar beamsplitters of various thicknesses have been employed to cover the complete infrared region. The experiments in the ultraviolet are performed at room temperature using a CARY spectrometer with an aluminium mirror as a reference.

3. Data analysis

The complex dielectric function cannot in general be derived directly from a measurement of the reflection. Only if the reflection is known over the complete frequency range can one calculate the dielectric response using the relations between the reflection and the phase derived from the Kramers–Kronig (KK) relations. The reflection spectrum of calaverite has been measured over a wide frequency range (see table 1); there are only three regions

missing in the data: (1) the low-frequency part below 20 cm^{-1}; (2) the near-infrared part between 5500 cm^{-1} and 14 000 cm^{-1}; and (3) the part above 47 000 cm^{-1}. For the low-frequency part one can assume the widely used Hagen–Rubens relation for the frequency dependence of the reflection given by $R = 1 - a\sqrt{\omega}$ to extrapolate the data to zero frequency. Since no structure is expected in the near-infrared region, one can interpolate the region between 5500 and 14 000 cm^{-1} using a smooth curve. A suitable function to interpolate this region is $R = a(1 - b\omega^2)$. The high-frequency part can be extrapolated using a suitable function which tends to zero for high enough frequencies. For this a function of the form $a\omega/(\omega^2 + b^2)^2$ is used, with the derivative matched to the high-frequency part of the available data. The neglect of any additional structure in this region, due for instance to atomic transitions, will not lead to changes in the positions of spectral features in the calculated optical spectra, but will merely lead to an error in the absolute intensities, which are not of particular interest here.

Table 1. Overview of the measured and inter-/extrapolated regions of the reflection of calaverite recorded using the given reference materials at temperature T and angle of incidence θ_i. Also listed are the most relevant excitations which contribute in the given regions as well as the inter-/extrapolation methods used.

Region (cm^{-1})	T (K)	θ_i	Excitations	Reference, extrapolation
0–20	—	—	—	$1 - a\sqrt{\omega}$
20–150	20	45	phonons	gold
150–5500	20	45	free electrons	gold
5500–14 000	—	—	—	$a(1 - b\omega^2)$
14 000–47 000	300	0	bound electrons	aluminium
47 000–10^6	—	—	—	$a\omega/(\omega^2 + b^2)^2$

Figure 1 shows the measured (11 200 points, full curves) and extrapolated parts (6500 points, broken curves) of the reflection as a function of frequency. The reflection shows a metallic behaviour with some phonon structure at low frequency, and a dip due to interband transitions just above 0.1 eV. The sharp peak at 5.2 eV in the spectrum probably is due to transitions from the Au 5d states in calaverite. These transitions have also been observed in XPS experiments at 5 eV [14]. The fluctuations in the spectrum around 0.1 eV are caused by interference effects in the spectrometer.

The dielectric function calculated using a KK analysis is shown in figure 2. The various vibrational and electronic excitations contributing to the dispersion of the dielectric function will be discussed in the next paragraphs.

4. Absorption by phonons

The average structure of calaverite has three atoms per primitive cell. Although there are nine phonon modes in this structure, the selection rules predict only three of them to be infrared active [2]. Due to the incommensurate modulation, however, one expects that not only phonons with momentum $k = 0$ are active, but also those with $k = \pm lq$ ($l = 1, 2, \ldots$) in optical scattering experiments [15]. This has already been confirmed in Raman experiments where 18 additional modulation induced modes have been observed [2]. In principle all phonons with $k = \pm lq$ ($l = 1, \ldots, \infty$) contribute to the optical scattering. However, their activity strongly depends on the number of harmonics which are needed to

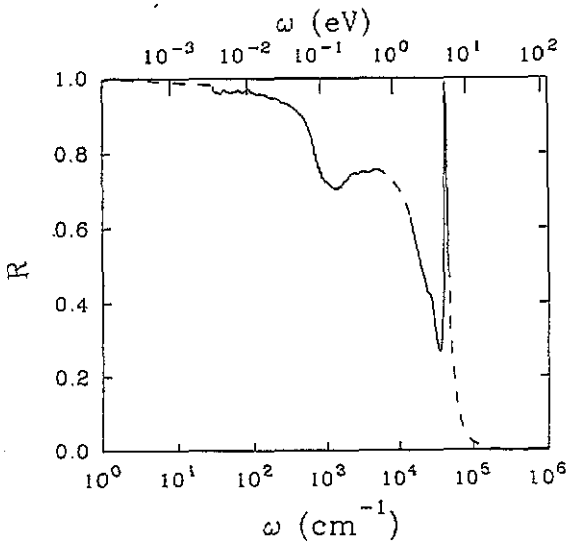

Figure 1. Frequency dependence of the reflection of calaverite. The full and broken curves show the measured data and the inter- and extrapolated data, respectively (see text).

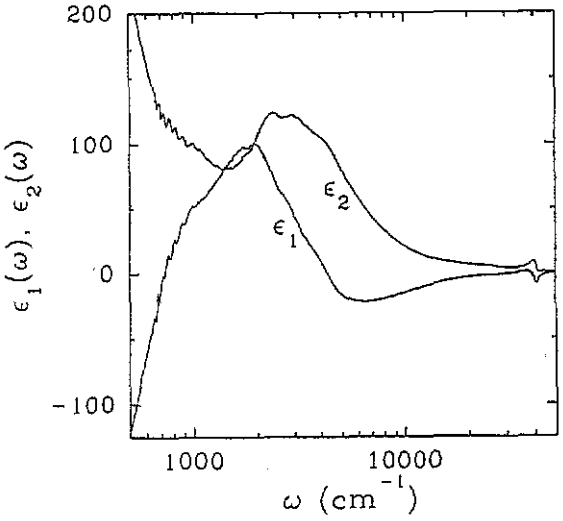

Figure 2. Real (ϵ_1) and imaginary (ϵ_2) parts of the dielectric function of calaverite calculated using a KK analysis from the reflection data shown in figure 1.

adequately describe the structure. It is usually sufficient to take into account only those phonons with low values of l. In the case of calaverite the selection rules predict that in addition to the three phonons for $l = 0$ an additional nine modes are expected for each value of l taken into account [2]. The Raman experiments showed that phonons with $l = 1, 2$ contribute to the optical scattering. If the same holds for infrared absorption one expects 21 active modes in the spectra.

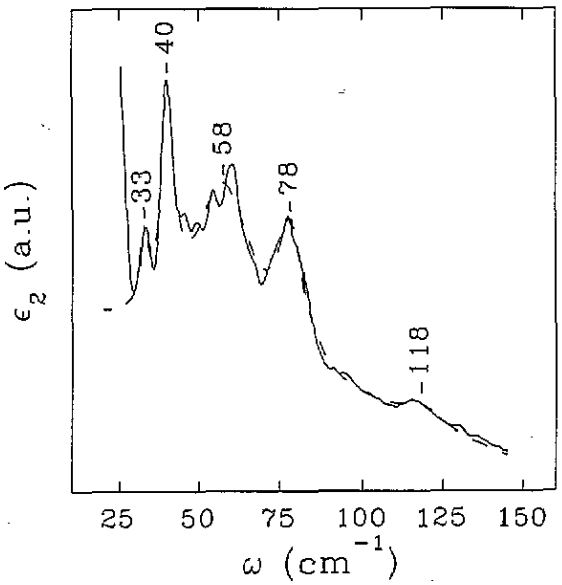

Figure 3. Low-frequency part of the imaginary part of the dielectric function showing activity of several phonons (full curve). The broken curve is a fit of Lorentzian-shaped peaks to the data (see text) whose peak frequencies are indicated at the markers.

Phonon scattering contributes to the reflection spectrum of calaverite in the region below 150 cm^{-1}. The imaginary part of the dielectric function derived from the reflection spectrum showing the phonon structure is shown in figure 3 (full curve). The fact that more than three phonons are observed clearly demonstrates the influence of the incommensurability in the optical spectrum. At least five reproducible modes are observed. The phonon contribution to ϵ_2 can be described using the Lorentz model for absorption by a harmonic oscillator. The spectral dependence of the absorption within this model is given by

$$\epsilon_2 = \sum_j \frac{S_j \gamma_j \omega}{(\omega_{0j}^2 - \omega^2)^2 + \gamma_j^2 \omega^2} \simeq \sum_j \frac{S_j \gamma_j/(4\omega_{0j})}{(\omega_{0j} - \omega)^2 + (\gamma_j/2)^2} \qquad \text{for } \gamma_j \ll \omega_{0j} \tag{1}$$

where S_j is the oscillator strength, ω_{0j} the resonance frequency, and γ_j the linewidth. The broken curve in figure 3 represents a fit of five Lorentzians to the data. A linear background was assumed in the fitting procedure to account for the absorption due to other processes. The resonance frequencies of the fitted Lorentzians are 33, 40, 58, 78, and 118 cm^{-1}, respectively. There seems to be more structure in the data and the peaks at 58 and 78 cm^{-1} may be split into more components. This additional structure does not reproduce very well and has therefore been neglected.

Since there are more phonons active than expected for the average structure of $AuTe_2$, one can conclude that the incommensurability has a strong effect on the vibrational absorption spectrum of $AuTe_2$. The selection rules for the incommensurate structure predict the activity of 12 ($l = 0, 1$) or 21 ($l = 0, 1, 2$) phonon modes. In Raman scattering it has been possible to observe most of these modes [2]. Clearly the infrared spectrum shows only some of the predicted modes. In the low-frequency region this is probably due to the broad linewidth of the observed bands in the infrared spectrum, leaving many of the expected modes unresolved. One expects from the Raman data to observe modes above 120 cm^{-1}. The infrared spectrum, however, does not show any reproducible structure in this region. The precise origin of this difference is at present not known, but it may be related to a decreasing skin depth with increasing frequency, leading to a decreasing sensitivity to phonon structure.

5. Absorption by electrons

The most important electronic processes which contribute to the dispersion of the dielectric function are absorptions due to interband and intraband transitions. It is often convenient to distinguish between these two processes in discussing the electronic scattering. Therefore this section starts with a discussion of the contribution of intraband transitions to the imaginary part of the dielectric constant. In the second part of this section the contribution of the interband transitions are discussed.

5.1. Intraband processes

Figure 4 (full curve) shows the imaginary part of the dielectric function as obtained from the KK analysis. The steep increase of ϵ_2 towards low frequencies is due to the intraband processes. The frequency dependence of the dielectric function in a metal can be understood in terms of the Drude free electron model. Within this model the dielectric function is given by

$$\epsilon_1(\omega) = \epsilon_\infty[1 - (\omega_p^2\tau^2/\epsilon_\infty)/(1+\omega^2\tau^2)] \tag{2}$$

$$\epsilon_2(\omega) = \omega_p^2\tau/\omega(1+\omega^2\tau^2) \tag{3}$$

where ϵ_∞ is the high-frequency limit of the dielectric constant if the interband transitions are neglected, τ the electronic intraband scattering time, and ω_p the plasma frequency.

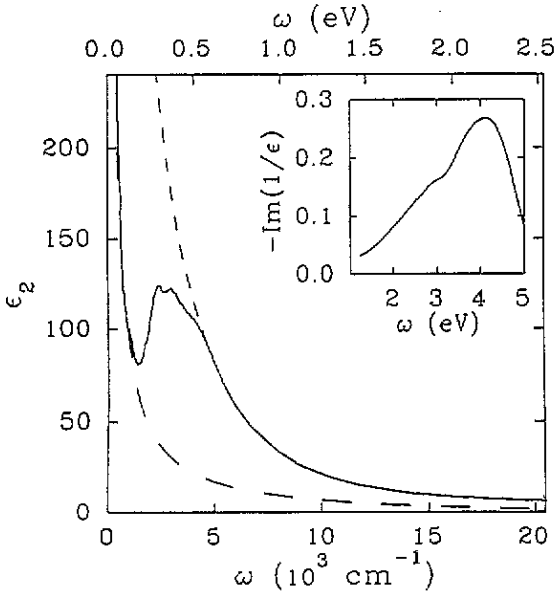

Figure 4. Imaginary part of the dielectric function (full curve). The long-dashed curve gives the Drude behaviour as derived from the plasmon peak in the loss function shown in the inset. The short-dashed curve gives a Drude-like fit to the tail of the interband transitions.

Before discussing the data in terms of the Drude behaviour it is interesting to first consider the low-frequency limit of the Drude behaviour, i.e. the DC conductivity $\sigma(0)$. This can be estimated from an extrapolation of the real part of the optical conductivity

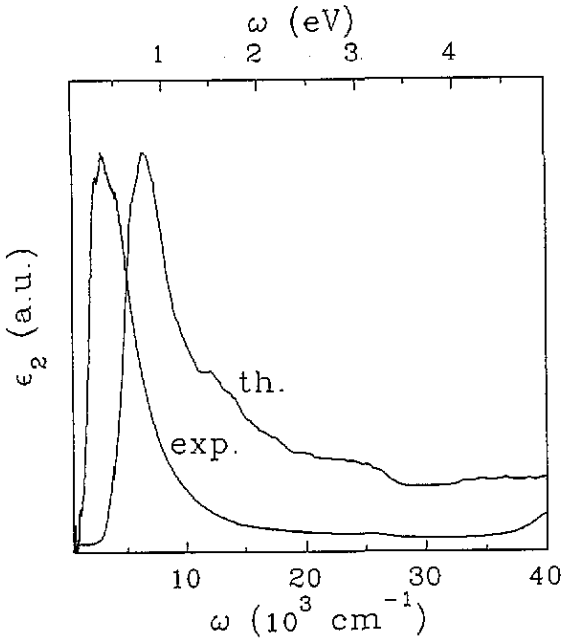

Figure 5. Contribution of the interband transitions to ϵ_2 obtained after subtraction of the Drude contribution ('exp.'). The curve marked 'th.' shows the results for ϵ_2 as calculated in [18].

$\sigma(\omega) = \omega\epsilon_2/4\pi$ to zero frequency, yielding $\sigma(0) \simeq 1$ $\mu\Omega$ m^{-1}. This is in relatively good agreement with the value of 2 $\mu\Omega$ m^{-1} at $T = 20$ K determined from resistance measurements, giving confidence in the results of the KK analysis.

Dijkstra *et al* [3] measured, using ellipsometry, the dielectric function of calaverite for 1.5 eV $< \hbar\omega <$ 5 eV. The present data agree with their results to within 5%, giving confidence in the results of the KK analysis. The ellipsometry data were interpreted in terms of a Drude model, with the Drude parameters given in table 2. It is obvious from the present data, however, that interband scattering rather than free electron scattering gives the largest contribution to ϵ_2 for energies above 1.5 eV. The characteristic Drude-like free electron contribution is found to be prominent at much lower energy ($\hbar\omega < 0.2$ eV). Since free electron scattering is important in a small energy range only it is difficult to fit the data directly to a Drude behaviour. One can, however, obtain a good estimate of the parameters of the Drude behaviour from the energy dependence of the loss function, defined as $-\mathrm{Im}(1/\epsilon)$, which is shown in the inset of figure 4. This function peaks at the position ω_c where ϵ_1 is zero, and has a full width of $\Delta\omega = 1/\tau$ [16]. Within the Drude model the frequency ω_c is related to the plasma frequency through $\omega_p^2 = \epsilon_\infty(\omega_c^2 + 1/\tau^2)$. Thus from a determination of the peak width and peak frequency of the loss function, one can in combination with the high-frequency limit of the dielectric constant obtain a good estimate of the characteristic parameters of the free electron scattering ω_p and τ. The broken curve in figure 4 (long dashes) gives the Drude behaviour calculated from the values obtained in this way (see table 2). From the agreement with the data one can conclude that the free electron contribution can be approximated by a Drude behaviour having a plasma frequency $\hbar\omega_p = 4.8$ eV and a characteristic scattering time $\tau = 3.2 \times 10^{-16}$ s. The electron density estimated from the plasma frequency $\omega_p = \sqrt{ne^2/m^*\epsilon_0}$, substituting the free electron mass

Table 2. Comparison of the plasma frequency and scattering time derived here to the results of [3]. ϵ_∞ gives the high-energy limit of the dielectric constant. $d\epsilon_2$ gives the 'background' assumed in [3].

	ω_p (eV)	τ (10^{-16} s)	ϵ_∞	$d\epsilon_2$
Drude	4.8	3.2	1.03	—
[3]	7.5	4.0	—	3.00

m_0 for the effective mass m^*, is $n \simeq 2 \times 10^{28}$ m^{-3}, a value typical for metals.

5.2. Interband processes

The contribution from interband processes to ϵ_2 can be found by subtraction of the Drude behaviour from the data presented in figure 2. As shown in figure 5 (curve marked 'exp.'). The interband contribution peaks at 0.4 eV, having a peak width of 0.5 eV. Krutzen [17] has performed electronic band structure calculations for commensurate approximants of $AuTe_2$. From these results the interband part of ϵ_2 has been calculated [18], assuming equal matrix elements for all interband transitions. For comparison these results are also shown in figure 5 (curve marked 'th.'). The predicted interband contribution peaks at 0.8 eV and has a bandwidth of 0.65 eV. These theoretical results overestimate the experimentally found values by a factor of 1.3 to 2. There could be several reasons for this discrepancy. It might be due to the partial neglect of the incommensurability in the electronic structure calculations for calaverite, i.e. due to the neglect of the possible existence of minigaps at the Fermi surface, leading to an overestimate of the onset of the interband transitions. In that case, one would also expect to observe structure in the low-energy tail of the interband contribution, which is evidently not the case. The agreement of the structure observed near the peak in both the experimental and theoretical spectra suggests that the discrepancy can be resolved by shifting the theoretical spectrum towards lower energy, i.e. the theoretical Fermi-energy has to be shifted. The theoretical overestimate of the peak width and the magnitude of the high-energy tail then results from a neglect of the energy dependence of the transition matrix elements. This leads to the conclusion that the matrix elements in general decrease with increasing energy.

It seems surprising that Dijkstra *et al* [3] could fit their data with a Drude-like behaviour. Also, for the present data it is possible to fit the high-energy tail of the interband contribution with a Drude-like behaviour, giving a 'scattering time' $\tau = 8.1 \times 10^{-16}$ s^{-1} and a 'plasma frequency' of 7.8 eV (see figure 4, broken curve (short dashes)). This Drude-like high-energy behaviour of the interband contribution may be due to the very rich, and relatively dense, bandstructure of calaverite [17]. For this kind of bandstructure one expects that for high enough energy, where the details of the bandstructure are no longer important and there are many final states, the contribution of interband processes to the optical spectrum will show a spectral dependence more or less similar to that expected for free electron processes [19]. It should be noted, however, that $\omega_p$and τ are parameters which strongly depend on the details of the bandstructure, and are not simply related to a real scattering time or electron density.

6. Concluding remarks

The data presented here show good agreement with the ellipsometry data of Dijkstra *et al* [3]. From this, and the good agreement found with the DC conductivity, one can conclude that KK

analysis yields sensible results. However, the data set used contains some inconsistencies which lead to errors in the derived optical spectra. In particular, the data below 0.7 eV have been measured at 45° incidence, unpolarized light has been used in the experiments, a rather arbitrary interpolation function has been used for the 0.7–1.7 eV region, and the UV data have been measured at room temperature. One can expect, however, that these deficits lead primarily to an error in the absolute values, and do not strongly affect the spectral dependence of the dielectric function.

Calaverite is usually considered to be a semi-metal. The results here show that synthetic pure $AuTe_2$ is a conductor with a DC conductivity and a Drude scattering time typical for semi-metals. The electron density $n \approx 2 \times 10^{28}$ m^{-3} of pure $AuTe_2$, estimated from the low-frequency Drude behaviour, is typical for a metal. For an incommensurately modulated conductor the combination of a semi-metallic conductivity with a metallic density may be not so surprising. If the modulation induces Fermi-surface nesting for wave vectors $\boldsymbol{k} = \pm l\boldsymbol{q}$, leading to a distribution of minigaps at or near the Fermi surface, one can expect that the inelastic scattering time of the conduction electrons strongly decreases, resulting in a decreased conductivity. However, since the electron density estimate depends crucially on the effective electron mass m^* in calaverite this cannot be concluded from the present data alone. It seems therefore interesting to determine the effective mass for calaverite, for instance from magneto-conduction experiments.

One expects that the existence of a contribution of minigaps also leads to a contribution to the interband scattering, with an absorption edge at the largest gap induced for $\boldsymbol{k} = \pm\boldsymbol{q}$. If this gap indeed exists in calaverite its magnitude is smaller than 60 meV, since no structure is observed in the low-energy tail of the interband contribution shown in figure 5 above this energy. For a definitive conclusion a careful analysis of the low-energy part of the spectrum is needed. The present data do not allow for this, and moreover do not extend to low enough energies.

To summarize, the incommensurate modulation of $AuTe_2$ is reflected in the optical absorption spectrum by the activity of additional phonons with wave vector $\boldsymbol{k} = \pm l\boldsymbol{q}$ ($l \neq 0$). The free electron scattering in this semi-metal can qualitatively be described with a Drude model ($\omega_p = 4.8$ eV, $\tau = 3.2 \times 10^{-16}$ s). The Drude parameters derived in [3] describe the tail of the interband scattering, which main contribution to the optical spectra is centred around 0.4 eV. The combination of semi-metallic conductivity with a metallic electron density gives an indication for a modulation induced Fermi-surface nesting in calaverite, though additional experimental research is needed for a definitive conclusion. The onset of the interband contribution to the optical spectrum sets an upper limit for the energy gaps of 60 meV.

Acknowledgments

One of the authors (KB) wishes to thank the Conselho Nacional de Pesquisa (CNPq, Brazil) for financial support (project 200644/88.2). Part of this work was financed by the Stichting Fundamenteel Onderzoek der Materie (FOM, The Netherlands).

References

[1] Dam B, Janner A and Donnay J D H 1985 *Phys. Rev. Lett.* **55** 2301
[2] van Loosdrecht P H M, van Bentum P J M and Balzuweit K 1992 *Ferroelectrics* **125** 517
[3] Dijkstra E, Kremers M and Devillers M A C 1989 *Z. Phys.* B **76** 487

[4] Schutte W J and de Boer J L 1988 *Acta Crystallogr.* B **44** 486
[5] Tunell G and Pauling L 1952 *Acta Crystallogr.* **5** 375
[6] Balzuweit K, Hovestad A, Meekes H and de Boer J L *J. Cryst. Growth* submitted
[7] Reithmayer K, Steurer W, Schulz H and de Boer J L 1990 *Proc. XVth CUIC (Bordeaux, 1990)*
[8] Tsuei C C and Newkirk L R 1969 *Phys. Rev.* **183** 619
[9] Meekes H, van Loosdrecht P H M and Kremers M 1990 unpublished
[10] de Lange C and Janssen T 1983 *Phys. Rev.* B **28** 195
[11] Barker A S and Ditzenberger J A 1970 *Phys. Rev.* B **1** 4378
[12] Meekes H 1988 *Phys. Rev.* B **38** 5924
[13] Balzuweit K, Meekes H and Bennema P 1991 *J. Phys. D: Appl. Phys.* **24** 203
[14] van Triest A, Folkerts W and Haas C 1990 *J. Phys.: Condens. Matter* **2** 8733
[15] Janssen T 1979 *J. Phys. C: Solid State Phys.* **12** 5381
[16] Raether H 1990 *Excitations of Plasmons and Interband Transitions by Electrons* (Berlin: Springer)
[17] Krutzen B C H 1990 *J. Phys.: Condens. Matter* **2**
[18] Krutzen B C H and Kremers M 1990 *Ferroelectrics* **105** 559
[19] Ehrenreich H and Philipp H R 1962 *Phys. Rev.* **128** 1622